Journal of Luminescence 186 (2017) 144–151

Contents lists available at ScienceDirect

Journal of Luminescence

journal homepage: www.elsevier.com/locate/jlumin

Electronic structure and luminescence properties of self-activated and Eu^{2+}/Ce^{3+} doped $Ca_3Li_{4\text{-}y}Si_2N_{6\text{-}y}O_y$ red-emitting phosphors

Quansheng Wu [a,b], Jianyan Ding [a,b], Yanyan Li [a,b], Xicheng Wang [a,b], Yuhua Wang [a,b,*]

[a] Key Laboratory for Special Function Materials and Structural Design of the Ministry of the Education, China
[b] Department of Material Science, School of Physical Science and Technology, Lanzhou University, Lanzhou 730000, China

ARTICLE INFO

Article history:
Received 21 April 2016
Received in revised form
14 January 2017
Accepted 6 February 2017
Available online 7 February 2017

Keywords:
Nitride
Phosphor
Photoluminescence
Red-emitting

ABSTRACT

The undoped and Eu^{2+}/Ce^{3+} doped $Ca_3Li_{4\text{-}y}Si_2N_{6\text{-}y}O_y$ ($0 \le y \le 1.5$) (CLSN) were successfully prepared by solid-state reaction and their luminescence properties were studied. The undoped CLSN shows red defect-related luminescence with maximum emission intensity at 710 nm, Eu^{2+} and Ce^{3+} doped CLSN also show red emission centered at 702 nm and 673 nm, respectively. The electronic structure and the thermal stability of CLSN were investigated in this work. The results indicate that CLSN:Eu^{2+}/Ce^{3+} could be conducive to the development of phosphor-converted light-emitting diodes.

1. Introduction

In recent years, phosphor-converted light-emitting diodes (pc-LEDs) are known as the fourth generation of light source. Compared with traditional light sources (incandescent and fluorescent lamps), LEDs exhibit the advantages of energy saving, environmental protection, and high efficiency, and can be widely used in various applications, for instance in displays, decorations, general lighting and other fields [1–7]. In pc-LEDs, phosphors are one of the key materials, which are used in combination with blue or near-ultraviolet LED chips to produce white light. Nitride/oxynitride phosphors, such as $MSi_2O_2N_2$ (M=Ca, Sr, Ba) [8,9], $M_2Si_5N_8$:Eu^{2+}(M=Ca, Sr, or Ba) [10], $MAlSiN_3$:Eu^{2+}(M=Ca, Sr) [11,12] and Eu^{2+}-, or Ce^{3+}-doped α-SiAlONs [13], have been extensively investigated due to their excellent luminescence properties (small thermal quenching and high quantum efficiency). Although large numbers of nitride/oxynitride phosphors have been researched for use in solid state lighting, a very limited number of them can be applied to pc-LEDs practically. Therefore, it is still necessary to research on the development of new phosphors.

Recently, there has been a growing focus on research into lithium containing nitrides (M-Li-Si/Al-N, M=Ca, Sr, Ba) for use as luminescent materials, such as Sr[$LiAl_3N_4$], [14] Ca[$LiAl_3N_4$], [15] $Ba_2LiSi_7AlN_{12}$, [16] and Ba[$Li_2(Al_2Si_2)N_6$] [17]. All of them exhibited a narrow-band red (blue, green)-emission. Especially for Sr[$LiAl_3N_4$]:Eu^{2+}, which is a narrow-band red-emitting phosphor with high thermal quenching temperature and high quantum efficiency. For lithium containing nitrides, LiN_4 tetrahedra and Si(Al)N_4 tetrahedra can be combined vertex-shared or edge-shared with each other. This combination generates a nitridometallate framework of Si/AlN_4 tetrahedra with M (M=Li, Ca, Sr, Ba) cations occupying the empty spaces [4,14]. The higher degree of condensation leads not only to an increased stability of the materials, but also to a high rigidity of the host lattice, and to a limited local structural relaxation of the Eu^{2+}/Ce^{3+} site in its excited state – a prerequisite for the desired small stokes-shifted, narrow-band emission [18].

$Ca_3Li_4Si_2N_6$ is a quaternary lithium nitridosilicate with isolated [Si_2N_6] ions which was first reported by Schnick and his coworkers in 2009 [Angewandte Chemie] [23]. The crystal structure of CLSN is built up from corner-shared 'bow tie' units of [Si_2N_6] and [Li_2N_6], yielding a high degree of condensation (κ=1, κ=atomic ratio (Si, Li):N). However, they only reported on the synthesis and structural features of $Ca_3Li_4Si_2N_6$ synthesized by using flux methods. The luminescence properties of self-activated and Eu^{2+}/Ce^{3+} activated $Ca_3Li_{4\text{-}y}Si_2N_{6\text{-}y}O_y$ ($0 \le y \le 1.5$) (CLSN) and the relation between the crystal structure and the luminescent properties have never been reported. In this work, we have successfully synthesized the self-activated and Eu^{2+}/Ce^{3+} activated CLSN red phosphors by solid-state reaction. The electronic structure of CLSN has also been calculated by density functional theory (DFT) methods [19–22].

---

[*] Corresponding author at: Department of Material Science, School of Physical Science and Technology, Lanzhou University, Lanzhou 730000, China.
E-mail address: wyh@lzu.edu.cn (Y. Wang).

http://dx.doi.org/10.1016/j.jlumin.2017.02.016
0022-2313/

Finally, the luminescence properties of self-activated and Eu^{2+}/Ce^{3+} activated CLSN have been investigated in detail.

2. Experiment section

2.1. Materials and synthesis

A series of lithium nitridosilicate phosphors, $Ca_{3-x}Li_{4-y}Si_2N_{6-y}O_y$:$xEu^{2+}$ (CLSN:xEu^{2+} $x=0$–0.05) and $Ca_{3-z}Li_{4-y-z}Si_2N_{6-y}O_y$:$zCe^{3+}$ (CLSN: zCe^{3+} $z=0$–0.05) ($0 \le y \le 1.5$), were synthesized by heating a stoichiometric mixture of Li_3N (Aldrich, >99.50%), Si_3N_4 (Aldrich, 99.5%), Ca_3N_2 (Aldrich, >95.0%), $CeCl_3$ (99.99%) and $EuCl_3$ (Aldrich, 99.999%) for 3 h to 900°C in a forming gas atmosphere (N_2:H_2=95:5). The starting materials were thoroughly ground in an agate mortar in a glovebox to form a homogeneous mixture. The concentrations of both moisture and oxygen in the glovebox were less than 1 ppm. The powder mixture was transferred into an Al_2O_3 crucible and heated to the target temperature at a rate of 15°C min^{-1} in a horizontal tube furnace. When the furnace was cooled to room temperature, the sintered products were ground again into powders for measurement. The title compound is not stable against air and moisture. The sample is placed in the ziplock bag in the Powder X-ray Diffraction (XRD) and optical test.

2.2. Characterization

2.2.1. XRD

Powder diffraction data were collected on a Bruker D2 PHASER X-ray Diffractometer with graphite monochromator using Cu Kα radiation ($\lambda = 1.54056$ Å), 30 kV 15 mA.

2.2.2. Electronic structure calculations

The electronic structure of CLSN was calculated using DFT methods performed with the Cambridge Sequential Total Energy Package (GASTEP) code on the basis of the single crystal structure of $Ca_3Li_4Si_2N_6$. The source of this crystal structure was reported by Wolfgang Schnick and his coworkers [23] 2009, The local-density approximations based on density functional theory were chosen for the theoretical basis of the density function.

2.2.3. Ultraviolet-visible (UV/vis) spectroscopy

The diffuse reflectance UV–vis absorption spectra were measured using a Perkin-Elmer 950 spectrometer, whereas $BaSO_4$ was used as a reference.

2.2.4. Luminescence

The photoluminescence (PL) and photoluminescence excitation (PLE) spectra were recorded at room temperature using a FLS-920T fluorescence spectrophotometer equipped with a 450 W Xe light source and double excitation monochromators. The emission spectrum was corrected for the spectral response of a monochromator and photomultiplier tube by a light diffuser and tungsten lamp. The excitation spectrum was also corrected for the spectral distribution of the xenon lamp intensity by measuring Rhodamine-B as reference. The PL decay curves were measured by a FLS-920T fluorescence spectrophotometer with an F900 nanosecond flash hydrogen lamp as the light source. High temperature luminescence intensity measurements were carried out using an aluminum plaque with cartridge heaters; the temperature was measured by thermocouples inside the plaque and controlled by a standard TAP-02 high temperature fluorescence controller.

2.2.5. Powders morphology

The powders morphology investigations were done using scanning electron microscopy (SEM; S-3400, Hitachi, Japan). The element composition was determined using an energy-dispersive X-ray spectroscopy (EDX) which was attached to the transmission electron microscopy (TEM, FEI Tecnai F30).

3. Results and discussion

3.1. Phase identification and morphology observation

The phase identification of CLSN phosphor characterized by XRD is shown in Fig. 1. As can be seen, both of the powder diffraction patterns are in good agreement with powder patterns reported in reference [23] and there is no detectable impurity phase presented, indicating that the CLSN samples are X-ray pure.

The SEM micrographs of CLSN, CLSN:0.005Eu^{2+} and CLSN:0.005Ce^{3+} are shown in Fig. 2a–f. Both of them exhibit an irregular-shaped morphology and the particles crystallize well. The particles exhibit a good dispersibility with a diameter of about 1–4 µm.

Apparently, small amounts of oxygen are quite inevitable in lithium nitridosilicates prepared by solid-state reaction using our method and the horizontal tube furnace. The raw materials of Li_3N and Si_3N_4 contain some oxygen content and a small amount of oxidation of raw materials cannot be avoided in the sintering process. Therefore, the phosphors CLSN:Eu^{2+}/Ce^{3+} prepared by using our method with the horizontal tube furnace would contain some oxygen. The corresponding EDX spectra analysis (Fig. 3) indicates that the product has a chemical composition of Ca, Si, N and O, as shown in Table 1. Li could not be detected by this method. So, the examined samples are actually expressed by the formula $Ca_3Li_{4-y}Si_2N_{6-y}O_y$ ($0 \le y \le 1.5$).

3.2. Electronic structures of CLSN

The DFT calculations of CLSN based on the crystal structure refinement are shown in Fig. 4. As exhibited in Fig. 4(a), the density of states of CLSN can be divided into three energy regions. The first region is located in the lower energy part (−10 to −50 eV) of the valence bands (VB), which is mainly composed of the Ca-3s3p, Li-1s, Si-3s3p and N-3s3p states. The second region with the energy ranging from −10 to 0 eV is close to the Fermi level (E_f). It can be observed that the N-2p states and Ca-3p states occupy the main part and hybridize with Si-3p states to build up the valence bonds, and the (Ca, Si)−3s states locating at −6 to −4.5 eV have little contribution to the valence bonds. The final region of conduction bands (CB) are mainly formed by the Ca-3d states and Si-3p states ranging from 2.8 eV to 6.75 eV, and N-2p

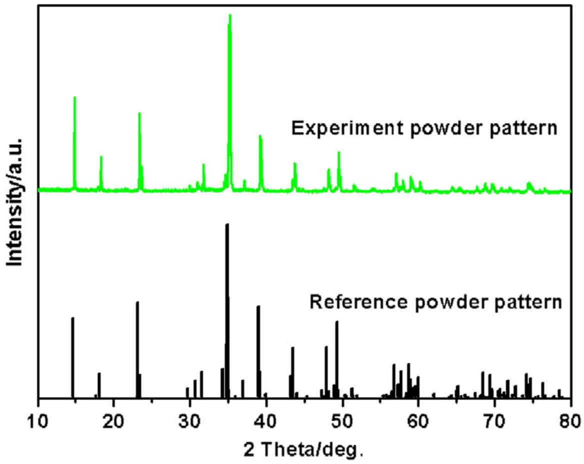

Fig. 1. XRD patterns of LCAN firing at 900 °C.